HHS Public Access

Author manuscript

Eur J Pharmacol. Author manuscript; available in PMC 2022 February 05.

Published in final edited form as:

Eur J Pharmacol. 2021 August 05; 904: 174123. doi:10.1016/j.ejphar.2021.174123.

New generation ENaC inhibitors detach cystic fibrosis airway mucus bundles via Sodium/Hydrogen Exchanger inhibition

Melania Giorgetti[a], **Nikolai Klymiuk**[b], **Andrea Bähr**[b], **Martin Hemmerling**[c], **Lisa Jinton**[c], **Robert Tarran**[d], **Anna Malmgren**[c], **Annika Åstrand**[c], **Gunnar C. Hansson**[a], **Anna Ermund**[a]

[a]Department of Medical Biochemistry and Cell Biology, University of Gothenburg, Sweden.

[b]Institute of Molecular Animal Breeding and Biotechnology, Gene Center, Ludwig-Maximilians-University Munich, Germany.

[c]Research and Early Development, Respiratory, Inflammation and Autoimmunity (RIA), BioPharmaceuticals R&D, AstraZeneca, Gothenburg, Sweden.

[d]Department of Cell Biology and Physiology, University of North Carolina at Chapel Hill, North Carolina, United States.

Abstract

Cystic fibrosis (CF) is a recessive inherited disease caused by mutations affecting anion transport by the epithelial ion channel cystic fibrosis transmembrane conductance regulator (CFTR). The disease is characterized by mucus accumulation in the airways and intestine, but the major cause of mortality in CF is airway mucus accumulation, leading to bacterial colonization, inflammation and respiratory failure. Several drug targets are under evaluation to alleviate airway mucus obstruction in CF and one of these targets is the epithelial sodium channel ENaC. To explore effects of ENaC inhibitors on mucus properties, we used two model systems to investigate mucus characteristics, mucus attachment in mouse ileum and mucus bundle transport in piglet airways. We quantified mucus attachment in explants from CFTR null (CF) mice and tracheobronchial explants from newborn CFTR null (CF) piglets to evaluate effects of ENaC or sodium/hydrogen exchanger (NHE) inhibitors on mucus attachment. ENaC inhibitors detached mucus in the CF mouse ileum, although the ileum lacks ENaC expression. This effect was mimicked by two NHE inhibitors. Airway mucus bundles were immobile in untreated newborn CF piglets but were detached by the therapeutic drug candidate AZD5634 (patent WO 2015140527). These results suggest that the ENaC inhibitor AZD5634 causes detachment of CF mucus in the ileum and airway via NHE inhibition and that drug design should focus on NHE instead of ENaC inhibition.

Corresponding author: Anna Ermund, Department of Medical Biochemistry and Cell Biology, University of Gothenburg, PO-Box 440, 405 30 Gothenburg, Sweden, Anna.Ermund@medkem.gu.se.

Author contribution statement

Conceptualization: A.M., A.Å., G.C.H. and A.E. Data curation: A.Å., G.C.H. and A.E. Formal analysis: M.G., N.K., L.J. and A.E. Funding acquisition: N.K., R.T., A.Å., G.C.H., and A.E. Investigation: M.G., N.K., L.J. and A.E. Methodology: M.G., N.K., A.B, M.H. and A.E. Project administration: N.K., R.T., A.B, M.H., A.M., A.Å., G.C.H., and A.E. Resources: N.K., A.B, M.H., R.T., A.M. and A.Å. Supervision: A.M., A.Å., G.C.H. and A.E. Validation: M.G., N.K., M.H., A.Å., G.C.H., and A.E. Visualization: A.E. Writing – original draft: M.G., N.K., M.H., L.J., A.Å., G.C.H., and A.E. Writing – review & editing: M.H., R.T., A.M., A.Å., G.C.H. and A.E.

Declaration of interest statement: Martin Hemmerling, Lisa Jinton, Anna Malmgren and Annika Åstrand are employees of AstraZeneca and may own stock or stock options. Martin Hemmerling is a co-owner of the patent WO 2015140527A1. Robert Tarran is a co-owner of patent US20170226180A1. The rest of the authors declare no competing interests.

Keywords

Mucus; Cystic fibrosis; Sodium/Proton exchanger; Trachea; Obstructive lung diseases; Epithelial sodium channel blockers

1. Introduction

Cystic fibrosis (CF) is a potentially fatal disease caused by function-disrupting mutations in the anion channel cystic fibrosis transmembrane conductance regulator (CFTR). In CF airways, mucus stagnation and accumulation lead to bacterial colonization, inflammation and ultimately tissue destruction and respiratory failure. The respiratory manifestations of CF are well recognized, whereas gastrointestinal complications are given less attention despite the fact that 15 to 20% of newborn babies with CF have meconium ileus (Sathe and Houwen, 2017) and a similar number of adults suffer from at least one life-time episode of distal intestinal obstruction syndrome (DIOS) (Colombo et al., 2011). Mucus accumulation and obstruction thus cause CF manifestations in both the airways and intestine. One explanation for these manifestations is decreased chloride and water secretion due to decreased CFTR function, linked to sodium hyperabsorption via the epithelial sodium channel (ENaC). However, this would not account for the effects in the ileum, where ENaC is not expressed. Therefore, mucus attachment is not completely explained by the sodium hyperabsorption theory. Using explants from mouse ileum mounted in horizontal Ussing-type chambers (Ermund et al., 2015a; Ermund et al., 2015b; Ermund et al., 2013; Gustafsson et al., 2012b) we have demonstrated the importance of bicarbonate transport via CFTR for the formation of normal, detached mucus in the ileum and linked the CF phenotype to CFTR dysfunction (Gustafsson et al., 2012a). Calcium ions and low pH are necessary to organize and pack mucin polymers in goblet cell secretory granules, enable secretion and tightly control the properties of the mucus as the same mucin can be easily moved or attached in different organs or conditions (Ermund et al., 2013). We studied mucus properties in WT and CF mouse ileum and realized that formation of normal, detached mucus was dependent on bicarbonate via CFTR (Ambort et al., 2012; Gustafsson et al., 2012a). Bicarbonate allowed sufficient expansion of the mucus to expose the cleavage site for the protease meprin B (EC 3.4.24.63, meprin β), the enzyme responsible for cleaving the secreted gel-forming mucin 2 (MUC2) and detaching the mucus. Lack of bicarbonate at mucus secretion in CF left the mucus more compact and hiding the cleavage site, thereby causing the attached CF mucus in the ileum (Schütte et al., 2014). Here we used the CF mouse ileum to demonstrate that the new generation ENaC inhibitors detach CF mucus in the ileum, despite lack of ENaC expression.

We have recently reported quantification of mucus bundle transport velocity in newborn piglet airway explants (Ermund et al., 2018; Ermund et al., 2017a). Using this model, we described how mucus bundles made from the secreted, gel-forming mucin 5B (MUC5B) expressed in airway submucosal glands (Trillo-Muyo et al., 2018) are coated by the secreted, gel-forming mucin 5AC (MUC5AC) and identified the importance of these mucus bundles in normal airway cleaning (Ermund et al., 2017a). In CF airways, mucus bundles are stagnant and attached to surface goblet cells (Ermund et al., 2018), indicating that

CFTR function is essential for mucus bundle movement in proximal airways. Alcian blue staining of mucus bundles in airway explants revealed a beneficial effect for the drug Atrovent® (ipratropium bromide, IUPAC name: [(1*R*,5*S*)-8-methyl-8-propan-2-yl-8-azoniabicyclo[3.2.1]octan-3-yl] 3-hydroxy-2-phenylpropanoate;bromide) on mucus bundle transport (Ermund et al., 2018), demonstrating the usefulness of this model in evaluating mucus active drugs. Inhibitors of ENaC are under development to improve mucus clearance in various lung diseases where mucus accumulation is a problem (Moore and Tarran, 2018) and most drug candidates are derivatives of the canonical ENaC inhibitor amiloride (IUPAC name: 3,5-diamino-6-chloro-*N*-(diaminomethylidene)pyrazine-2-carboxamide). In contrast, ENaC inhibition is achieved by internalization of ENaC from the cell surface by the peptide SPX-101 (IUPAC name: (3S)-4-[[(2S)-5-amino-1-[[(2S,3R)-1-[[(2R)-1-[[(2R)-1-amino-1-oxopropan-2-yl]amino]-1-oxopropan-2-yl]amino]-3-hydroxy-1-oxobutan-2-yl]amino]-1,5-dioxopentan-2-yl]amino]-3-[[(2S)-2-[[(2S)-1-[(2S,3S)-2-[[(2S)-1-[(2S)-2-[[(2R)-2-[[(2R)-2-aminopropanoyl]amino]propanoyl]amino]-4-methylpentanoyl]pyrrolidine-2-carbonyl]amino]-3-methylpentanoyl]pyrrolidine-2-carbonyl]amino]-4-methylpentanoyl]amino]-4-oxobutanoic acid (Scott et al., 2017). Here we quantified the effect of the therapeutic drug candidates AZD5634 ((patent WO 2015140527), Parion (patent application WO 2013/003386) and SPX-101 on mucus bundle movement in newborn CF piglet trachea in order to test the hypothesis that ENaC inhibition is not sufficient to detach CF mucus and increase airway mucus bundle transport.

2. Materials and methods

2.1. Ethical statement of animal experimentation

All experiments were carried out in accordance with the European Communities Council Directive 2010/63/ EU for the care and use of laboratory animals and the ARRIVE guidelines. Protocols for the mouse experiments were approved by the Swedish Laboratory Animal Ethical Committee in Gothenburg, Sweden (3006–2020) and protocols for pig experiments were obtained from Regierungen von Oberbauern, Munich, Germany (AZ55.2–1-54–2531-78–07) and Jordbruksverket, Jönköping, Sweden (Dnr 6.7.18–12708/2019).

2.2 Mice

Transgenic and wild type (WT) mice were housed in individually ventilated cages (maximal number 5 mice per cage) under controlled temperature (21–22° C), humidity and 12-h light/dark cycle under specific pathogen-free conditions. Homozygous $Cftr^{tm1UNC}$ null mice (RRID:CWRU_S) on C57BL/6 background were bred as heterozygotes at the University of Gothenburg, maintained as described (van Doorninck et al., 1995) and given regular water 5 days before the experiments. C57BL/6 mice (RRID:B6NTac) were used as WT controls. The WT mice were either purchased from Taconic or obtained from our in-house breeding program. Male and female mice aged 8–16 weeks were killed by cervical dislocation under isoflurane anesthesia.

2.3 Piglets

Homozygous male and female CFTR knock-out (CF) and wild-type littermate piglets were obtained by heterozygous breeding as described previously (Klymiuk et al., 2012). Births

were induced as described (Ermund et al., 2017a). Airways and lungs were explanted and immersed in chilled Perfadex® solution (XVIVO Perfusion, Gothenburg, Sweden) adjusted to pH 7.2 with 1 M Tris-buffered saline. All connective and pulmonary tissue were removed, the airways transferred to a 50 ml tube with Perfadex® solution and shipped at 4°C overnight to Gothenburg (World Courier).

2.4 Quantification of mucus attachment

Intestinal explants from the ileum of WT and $Cftr^{tm1Unc}$ (CF) mice on a C57BL/6 background were used to evaluate mucus attachment as described previously (Gustafsson et al., 2012a) using activated charcoal (C9157–2.5KG, Sigma-Aldrich, St. Louis, MO) to visualize the mucus surface. Mice were used due to the availability of genetic mouse models and the experimental approach was proven useful for evaluating mucus active drugs (Ermund et al., 2017b). Mounted tissue was heated to 37°C and perfused on the basolateral side with Krebs-glucose buffer (116 mM NaCl, 1.3 mM $CaCl_2$, 3.6 mM KCl, 1.4 mM KH_2PO_4, 23 mM $NaHCO_3$, 1.2 mM $MgSO_4$, 10 mM D-glucose, 5.1 mM Na-glutamate, and 5.7 mM Na-pyruvate), pH 7.4, gassed with 95% O_2/5% CO_2. On the apical side the chamber contained 150 µl Krebs buffer where glucose was substituted with 10 mM D-mannitol. For the bicarbonate-free solutions, $NaHCO_3$ was replaced by an equimolar concentration of Na-HEPES, the solution was gassed with 100% O_2, and the pH was adjusted to 7.4. In the buffer containing 115 mM bicarbonate, NaCl was replaced with an equimolar concentration of $NaHCO_3$, aerated with 95% O_2/5% CO_2 and the pH was then adjusted to 7.4. A thorough characterization of this buffer was published elsewhere (Gustafsson et al., 2012a). Drugs were incubated apically for 60 min on preformed mucus (mucus already formed when tissue was mounted) or after preformed mucus was removed. If preformed mucus had been removed, secretion of new mucus was stimulated by basolateral perfusion of 10 µM carbachol (C4382, Sigma-Aldrich, St. Louis, MO) and 10 µM prostaglandin E_2, (P5640–5MG, Sigma-Aldrich, St. Louis, MO) as described (Gustafsson et al., 2012a). Mucus thickness was measured from the mucus surface to the villi tips at 60 min. To evaluate mucus properties, the whole apical volume was aspirated using a plastic Pasteur pipette (Cellprojects, Sutton Valence, UK). The remaining mucus thickness was measured after refilling the apical chamber with 150 µl Krebs–mannitol and adding new charcoal particles (Ermund et al., 2017b). Finally, all mucus was removed and the villi height was measured from the epithelium between the villi to the villi tips. Mucus attachment is presented as percent removed, calculated from the mucus thickness before and after removal with the Pasteur pipette.

2.5 Microelectrode pH measurements

Ileum from WT and CF mice was mounted in the horizontal Ussing-type perfusion chamber, heated to 37°C, the basolateral side perfused with aerated (5% CO_2/95% O_2) Krebs-glucose buffer (composition in mM: 116 NaCl, 1.3 $CaCl_2$, 3.6 KCl, 1.4 KH_2PO_4, 23 $NaHCO_3$, 1.2 $MgSO_4$, 5.7 sodium pyruvate, 5.1 sodium-L-glutamate and 10 D-glucose, pH 7.4) at a rate of 5 ml/min and the apical surface submerged in 150 µl aerated (5% CO_2/95% O_2) Krebs-mannitol buffer with the same composition as the Krebs-glucose buffer, but with D-glucose substituted with the same concentration D-mannitol. WT and CF piglet trachea were mounted in a horizontal Ussing-type perfusion chamber heated to 37°C (Gustafsson

et al., 2012b), the basolateral side perfused with Krebs-glucose buffer at a rate of 5 ml/min and the apical epithelium submerged in 150 μl aerated (5% CO_2/95% O_2) HEPES-buffer (2 mM HEPES, 1.5 mM NaCl, pH 7.35). Surface pH was measured using a microelectrode with a tip diameter of 500 μm and a reference electrode, tip diameter 100 μm (PH-500, REF-100, Unisense, Aarhus, Denmark). The reference electrode was placed in the apical chamber 1 mm from the pH-sensing electrode and the pH-sensing electrode was placed on the epithelium as judged via a stereo microscope (Nikon Instruments, Melville, NY). The electrodes were calibrated using standard pH calibration buffer solutions (HI-7007L, HI-7004L, HI-7010L Hannah Instruments, Leighton Buzzard, UK). Compounds were added to the apical chamber and the pH always stabilized within three min. Then the measurement was registered.

2.6 Mucus bundle velocity quantification

Excised newborn wild type (WT) and $CFTR^{-/-}$ (CF) piglet distal tracheas and primary bronchi were incubated in Krebs-glucose buffer with inhibitors in Falcon tubes in the dark for two hours at ambient temperature. The distal trachea and primary bronchi were thereafter mounted in a chamber with aerated (5% CO_2/95% O_2) Krebs-glucose buffer (in mM: 116 NaCl, 1.3 $CaCl_2$, 3.6 KCl, 1.4 KH_2PO_4, 23 $NaHCO_3$, 1.2 $MgSO_4$, 5.7 sodium pyruvate, 5.1 sodium-L-glutamate and 10 D-glucose, pH 7.4) and heated to 37°C. Mucus was stained with 0.4 mM Alcian blue 8GX (A3157, Sigma-Aldrich, St. Louis, MO) in the same buffer. Transport of Alcian blue-stained mucus bundles was evaluated in time-lapses acquired with an SMZ18 stereomicroscope using NIS-Elements (Nikon Instruments, Melville, NY). Pig airways have submucosal glands down to the tenth generation of bronchi, as in humans and the cleaning of the large airways (> 2mm in diameter) is performed by mucus bundles made by submucosal glands, sweeping over the airways to collect bacteria and debris (Ermund et al., 2017a). Furthermore, access to CFTR null piglets enables testing of drug candidates for treatment of CF lung disease in a relevant CF model (Ermund et al., 2018).

2.7 Analysis of mRNA levels in piglets

Tissue from lung, kidney and colon were cut into pieces, directly frozen on dry ice and stored at −80°C. For RNA isolation, samples were powdered under liquid nitrogen. First, tissue was wrapped in pre-cooled tinfoil and crushed with a pre-cooled hammer on a pre-cooled anvil. Second, crushed tissue pieces were minced in a pre-cooled mortar with a pre-cooled pestle. Powdered tissue was then transferred into a pre-cooled tube and stored again at −80°C. RNA isolation was done with TRIzol Reagent (15596026, ThermoFisher Scientific, Carlsbad, CA). Approximately 100 mg of powdered tissue was homogenized in 1 ml Trizol using a Polytron PT2500E (Kinematica, Luzern, Switzerland) in a pulsatile manner to avoid overheating. Further steps were carried out according to the Trizol protocol and remaining genomic DNA was degraded by RNase-free DNase (EN0521, ThermoFisher Scientific, Carlsbad, CA). A total of 1.2 μg RNA was reverse transcribed by the SuperScript III kit (ThermoFisher Scientific, Carlsbad, CA). RT-PCR was performed with the primers for the ENaC subunits SCNN1A, SCNN1B, SCNN1C, the NHE exchangers SLC9A1 – SLC9A8, CFTR and the housekeeping genes GAPDH (Glyceraldehyde 3-phospate dehydrogenase), YWHAZ (14–3-3 protein zeta/delta) and TBP

(TATA binding protein), see table 1, and the Herculase II polymerase (600677, Agilent, Santa Clara, CA).

The same master mix, 5 μl 5x Buffer, 2.5 μl 2 mM dNTP, 0.4 μl of 10 μM primers, 15.5 μl H_2O, 0.2 μl enzyme, 1.0 μl cDNA and the same cycler protocol, 95°C for 4 min, 35 cycles of 95°C 20 s, 58°C for 20 s, 72°C for 30 s, and then 72°C for 5 min, 4°C for 5 min were used for all RT-PCRs. Electrophoresis was run on a 2.5 % agarose gel. For qPCR, cDNA quality was checked by serial dilution (1:16, 1:32, 1:64, 1:128, 1:256) for slope and correlation coefficient with the primers for the TBP housekeeping gene. Comparative delta-Ct analysis was then performed at the 1:32 dilution with the same primers as described for RT-PCR, except SLC9A2, SLC9A3 and SLC9A4 which appeared not expressed in the lung. The master mix was 6.25 μl FastStart Essential DNA Green Master (Roche Life Science, Basel, Switzerland), 0.75 μl Uracil-DNA glycosylase (ThermoFisher Scientific, Carlsbad, CA), 2.5 μl template, primers and H_2O up to a total volume of 12.5 μl. Optimal conditions were found to be 0.3 μl primers for YWHAZ, SCNN1G, SLC9A1, SLC9A6, SLC9A7, SLC9A8; 0.4 μl primers for SCNN1A, SCNN1B; 0.5 μl for CFTR and GAPDH; 0.7 μl for TBP. Assays were run on a LightCycler96 (Roche Life Science, Basel, Switzerland) following a temperature profile of 50°C for 2 min, 95°C for 10 min, 45 cycles of 95°C for 10 s, 63°C for 90 s, except for CFTR and GAPDH for which an elongation step for 60°C for 90 s was used. Data were analyzed on the LightCycler96 software (Roche Life Science, Basel, Switzerland), extracted and processed by Excel (Microsoft, Redmond, WA) and GraphPad Prism (GraphPad Software, San Diego, CA).

2.8 Drugs

Compound A, (*R*)-3,5-diamino-6-chloro-*N*-(3-(((1-(4-guanidinobutanoyl)piperidin-4-yl)methyl)amino)-2-(2-methylbenzyl)propyl)pyrazine-2-carboxamide (Åstrand et al., 2015) was selected from an AstraZeneca compound library of basic derivatives of 3,5-diamino-6-chloro-pyrazine-2-carboxamides that exhibit high selectivity and potent inhibitory activity (pIC_{50} 9.8) against ENaC, assessed in Ussing chamber experiments on human bronchial epithelial cells grown in air-liquid interface cultures. AZD5634 (patent WO 2015140527 by Berglund, S.E. et al.), structurally related to Compound A, is developed by AstraZeneca for the treatment of CF lung disease. The Parion compound is identical to Compound Ia from the patent application WO 2013/003386. Here, the presented effect on mucociliary clearance in sheep is apparently identical to the data revealed at the AIT-ISAM joint conference (Princeton, NJ, September 2014) for P-1037, also known as GS-5737 and VX-371. AZD5634 and Parion inhibit ENaC with similar potency and are about 10-fold less potent than Compound A (pIC_{50} 8.6 and 8.7, respectively). 5-(N,N-Dimethyl)amiloride hydrochloride (DMA, A4562–25MG, Sigma-Aldrich, St. Louis, MO) is an NHE inhibitor used to demonstrate that inhibition of NHE3 induces bicarbonate secretion in the small intestine (Furukawa et al., 2004; Repishti et al., 2001). AZ1607 (patent application WO 2014/169094) was made by Ardelyx (Fremont, CA) and is a close structural analog to Tenapanor (IUPAC name: 1-[2-[2-[2-[[3-[(4*S*)-6,8-dichloro-2-methyl-3,4-dihydro-1*H*-isoquinolin-4-yl]phenyl]sulfonylamino]ethoxy]ethoxy]ethyl]-3-[4-[2-[2-[2-[[3-[(4*S*)-6,8-dichloro-2-methyl-3,4-dihydro-1*H*-isoquinolin-4-yl]phenyl]sulfonylamino]ethoxy]ethoxy]ethylcarbamoylamino]butyl]urea), an

FDA-approved treatment for irritable bowel disease with predominant constipation. AZ1607 is described in patent application WO 2014/169094 as Compound 003 with pIC_{50} of 8.1 on human NHE3. Compound A, AZD5634 and Parion are derivatives of the canonical ENaC inhibitor amiloride (A7410–1G, Sigma-Aldrich, St. Louis, MO). SPX-101 is a synthetic dodecapeptide mimetic of the natural ENaC inhibitor short palate, lung, and nasal epithelial clone 1 (SPLUNC1). SPX-101 was made by fmoc solid state synthesis by AmbioPharm (Charleston, USA), described in the patent US20170226180A1 and the chemical structure was published previously (Scott et al., 2017). Concentrations were chosen based on published Emax values (Åstrand et al., 2015) for amiloride (100 μM), AZ1607 (300 nM) and Compound A (1 μM) and the same concentration (1 μM) was used for Parion and AZD5634. For SPX-101 we used the Emax value published in (Scott et al., 2017). The general anion-transport inhibitor 4,4'-Diisothiocyano-2,2'-stilbenedisulfonic acid (DIDS, 462268–100G, Sigma-Aldrich, St. Louis, MO) at 100 μM was used to demonstrate the importance of anion secretion for normal mucus properties. Compound A, AZD5634, AZ1607, SPX-101 and Parion were provided by AstraZeneca. Molecular structures are presented in fig. S1.

2.9 Statistical analysis

Data were acquired and quantified using NIS Elements (RRID:SCR_014329, Nikon Instruments, Melville, NY) or Microsoft Excel (RRID:SCR_016137, Microsoft, Redmond, WA) and GraphPad Prism version 8.2.1 (RRID:SCR_002798, GraphPad Software, San Diego, CA). All available animals were included and no samples were excluded in any of the animal experiments. Statistical analysis was always two-tailed and we used non-parametric tests when possible because we did not assume Gaussian distribution. For multiple comparisons Kruskal-Wallis with Dunńs multiple comparisons test was used. For paired tests, Wilcoxońs test was used. The statistical details of the experiments can be found in the figure legends, including the specific statistical tests used and the exact number of n. Differences were considered significant when $P < 0.05$.

3. Results

3.1 Attached CF mucus is detached by bicarbonate and NHE3 inhibition

The mucus in the mouse small intestine was easy to remove from WT explants mounted in a horizontal Ussing-type chamber (Fig. 1A). In contrast, CF mucus was attached and not removed by controlled aspiration (Fig. 1A). Mucus attachment was dependent on the capacity of CFTR to transport bicarbonate as removal of bicarbonate from the serosal buffer resulted in attached WT mucus. The importance of bicarbonate for detachment of mucus was further demonstrated when 115 mM bicarbonate in the apical buffer detached CF mucus (Fig. 1A), as reported (Gustafsson et al., 2012a).

As ENaC inhibition has been suggested as therapy for CF, we incubated explants from CF mouse ileum with the canonical ENaC inhibitor amiloride at 100 μM, as this concentration gave complete blockade of ENaC as used in nasal potential difference measurements (Rowe et al., 2011) and measured mucus thickness before and after controlled aspiration. The CF mucus remained attached (Fig. 1B). This was no surprise as amiloride sensitive short circuit

currents are absent in the ileum (Koyama et al., 1999) and mRNA encoding ENaC subunits are low (Fukushima et al., 2005).

We have demonstrated that small intestinal mucus detachment is dependent on bicarbonate on the mucosal side of the epithelium. Bicarbonate expands mucus by increasing the pH and removing Ca^{2+} from the granule-packed mucin. Therefore, we hypothesized that the increased bicarbonate concentration results in an increased surface pH. One family of ion channels regulating cellular pH is the sodium/proton exchangers (NHE; SLC9A). In the ileum, NHE3 (SLC9A3) is the most abundantly expressed proton transporter in the apical membrane of enterocytes and inhibition of NHE3 was demonstrated to result in increased bicarbonate concentration in the duodenum (Repishti et al., 2001; Turner et al., 2000). To test our hypothesis that NHE3 inhibition was important for the detachment of CF mucus, we incubated CF ileum apically with the NHE inhibitor 5-(*N*,*N*-Dimethyl)amiloride (DMA at 100 μM for optimal NHE inhibition). The CF mucus was detached and made as easily removable as WT mucus (Fig. 1B). As we previously demonstrated, secretion of bicarbonate at the apical epithelial membrane was essential for detachment of mucus (Gustafsson et al., 2012a). Thus, we preincubated mounted ileal tissue apically with 4,4'-Diisothiocyano-2,2'-stilbenedisulfonic acid (DIDS at 100 μM), a general inhibitor of anion transport and then treated the explants with DMA. This treatment prevented mucus detachment by DMA, confirming that DMA detaches mucus via an apical anion secretion mechanism (Fig. 1B). To further characterize the effect of DMA, we perfused the explants on the serosal side with a bicarbonate-free buffer (Gustafsson et al., 2012a) while incubating with DMA. The lack of bicarbonate had the same effect as DIDS, reversing the mucus detachment caused by DMA (Fig. 1B). To further test our hypothesis, we incubated CF ileum explants apically with the NHE3 inhibitor AZ1607 (300 nM). The compound detached CF mucus, similar to DMA but with higher potency and the effect was also reversed by apical DIDS (Fig. 1C). Apical DIDS alone did not detach CF mucus. Compound structures are presented in Fig. S1. Taken together, these results indicated that small intestinal mucus detachment was bicarbonate secretion-dependent and that NHE inhibition caused CF mucus detachment in the ileum.

3.2 New generation ENaC inhibitors detach CF mucus in the mouse ileum

The canonical ENaC inhibitor amiloride has been shown by others to inhibit some NHEs (Masereel et al., 2003) when applied at concentrations above 100 μM and since the amiloride molecular structure was used as a starting point to develop new generation ENaC inhibitors, we hypothesized that these compounds inhibit NHEs. Following up on our result that a selective NHE3 inhibitor (AZ1607) detached CF mucus (Fig. 2A), we analyzed the mucus detaching properties of new generation ENaC inhibitors in mouse ileum. Compound A was previously evaluated for its ability to inhibit ENaC (Åstrand et al., 2015). Here we show that ileal CF mucus was detached by Compound A at 1 μM (Fig. 2A). Similar to the effect of the NHE inhibitors DMA and AZ1607, the effect of Compound A was reversed by apical DIDS preincubation (Fig. 2A), indicating anion secretion dependence. Similarly, AZD5634 and Parion (both at 1 μM for maximum ENaC inhibition), detached ileal CF mucus (Fig. 2A). Thus, three ENaC inhibitors, Compound A, AZD5634 and Parion,

detached CF mucus, despite lack of ENaC in the ileum (Fukushima et al., 2005; Koyama et al., 1999).

To further address the mechanism of action of these new generation ENaC inhibitors, we used microelectrodes to measure the pH in mucus on mouse ileal explants mounted in the same horizontal Ussing-type chamber heated to 37°C used for mucus thickness measurements (Gustafsson et al., 2012b). Krebs buffers gassed with 5%CO_2/95%O_2, with 10 mM glucose on the serosal side and equimolar mannitol on the mucosal side were used. The presence of a mucus layer covering the epithelial surface was evident as the pH was stable in the mucus but unstable when the probe was moved outside the mucus (Fig. 2B). Measurements were performed with the reference electrode in the bath, 1 mm from the pH-sensing electrode, which was placed on the epithelium. When compounds were added to the mucosal buffer, the pH stabilized within three min and the measurement was registered. As expected for an NHE3 inhibitor, AZ1607 increased the surface pH in both WT and CF ileum (Fig. 2C and D). Compound A also increased the pH in both WT and CF ileum to a similar extent as AZ1607, at a median around 0.3 pH units, which was consistent with NHE3 inhibition. However, there was no effect of AZD5634 on the surface pH in either WT or CF mouse ileum. As with mucus detachment, amiloride had no significant effect on pH. The Parion compound increased the pH in WT ileum, but there was no effect in CF ileum (Fig. 2C and 2D).

3.3 Newborn piglet airways are cleared by mucus bundles and express NHE mRNA

To explore the potential of ENaC inhibitors for inhaled therapy, we studied their effects in a CF piglet airway model, and we quantified mucus bundle transport as described (Ermund et al., 2017a). The distal trachea and primary bronchi were mounted in a chamber heated to 37°C and placed on a tilted holder. The mucus was stained by Alcian blue in physiological buffer (Fig. 3A). Using this method, we observed mucus bundles transported cephalically and sweeping over the airway surface to collect bacteria (Ermund et al., 2018; Ermund et al., 2017a). We have shown that mucus bundles in CF piglet airways are almost immobile (Fig. 3B), suggesting that CF disease starts at birth (Ermund et al., 2018). We also quantified the mRNA expression of *CFTR*, ENaC subunits *SCNN1A*, *SCNN1B* and *SCNN1G*, *SLC9A1–4* and *SLC9A6–8* by reverse transcriptase (RT)-PCR (Fig. S2) and qPCR on RNA prepared from isolated WT and CF lung tissue. The relative mRNA levels were calculated relative the housekeeping gene TBP. We could detect CFTR mRNA in WT piglet lung, but not in CF piglet lung, confirming the genotype and providing both a positive and negative control for the technique. Furthermore, the three ENaC subunits were expressed equally in WT and CF lungs. As expected, the ubiquitous basolateral sodium/proton exchanger NHE1 encoded by the gene *SLC9A1* and responsible for regulating intracellular pH had the highest expression (Fig. 3C) (Hasselblatt et al., 2000). We were unable to detect *SLC9A2, 3* or *6* in piglet lungs whereas they were present in kidneys and/or colon as analyzed by RT-PCR (Fig. S2). The NHEs encoded by *SLC9A6, 7* and *8* were detected in both WT and CF piglet lung to equal levels, with the exception of *SLC9A8*, which was expressed at a higher level in CF than WT tissues (Fig. 3D).

3.4 New generation ENaC inhibitors increase mucus bundle transport in CF piglet trachea

All ENaC inhibitors that we tested detached CF mucus in the ileum. However, as these are candidate therapies for CF lung disease, we assessed them in our newly described piglet model for airway mucus bundle transport (Ermund et al., 2017a). Compound A increased the transport of CF mucus bundles to velocities comparable to WT pretreated with Compound A. This effect was inhibited by DIDS as in the mouse ileum (Fig. 4A). The effect of Compound A was significant also when comparing means per pig (Fig. 4B). These results indicated a mechanism involving secretion of anions to detach mucus separate from ENaC inhibition also in the airways. The Parion ENaC inhibitor had no effect on mucus transport in CF piglet airways, neither at 1 μM nor at 10 μM (Fig. 4C). In contrast, the AstraZeneca compound AZD5634 significantly increased mucus bundle transport velocity in CF piglet airways to be comparable with transport in WT airways at 10 μM (Fig. 4D). The lower concentrations of AZD5634 had no effect. Please note that the y-axes have different scales in C and D. On the other hand, the ENaC inhibitors SPX-101 (10 μM) and amiloride (100 μM) or the NHE3 inhibitor AZ1607 (300 nM) had no effect on airway mucus bundle transport (Fig. 4E).

3.5 New generation ENaC inhibitors increase surface pH in piglet trachea

To further investigate the mechanism of action in piglet airways, we measured surface pH using the same method as in the mouse ileum. As the airway epithelial surface is not covered by a mucus layer but a thin liquid layer, pH studies were more difficult to perform as the pH was found to be more unstable. To validate our method, we measured pH in WT and CF piglet airways and were able to confirm the previously demonstrated lower pH in CF compared to WT piglet airways (Fig. 5A) (Simonin et al., 2019). Mucosal incubation with AZ1607 increased pH in WT but not CF airways. Compound A had no effect on WT pH (Fig. 5B) but increased the pH in CF (Fig. 5C). The AstraZeneca ENaC inhibitor AZD5634 was the only compound with effect in both WT and CF airways, with comparable pH increase. Amiloride increased surface pH in CF but not in WT piglet airways (Fig. 5B and C). These results show that the compounds with ability to increase CF piglet airway mucus bundle transport, Compound A and AZD5634, also increased surface pH in CF piglet airways.

4. Discussion

The present study highlights the potential for additional targets in the airways and ileum to be responsible for the mucus-detaching ability of some new generation ENaC inhibitors in development for treatment of CF lung disease. We have previously linked defective bicarbonate transport via CFTR to the attached mucus in CF (Gustafsson et al., 2012a) and identified Ca^{2+} as an important ion in mucus packing in goblet cell granules (Ambort et al., 2012). We have also identified Ca^{2+} chelation as the mechanism of action of the drug OligoG CF-5/20 (in clinical development for treatment of CF lung disease), indicating the importance of Ca^{2+} removal from the mucin for mucus expansion and detachment (Ermund et al., 2017b). New generation ENaC inhibitors are in development for treatment of muco-obstructive airway disease by several drug companies. We reasoned that hydration of airways *per se* will not detach stagnant CF mucus and decided to explore whether the new

generation ENaC inhibitors detach ileal CF mucus where ENaC is not expressed (Fukushima et al., 2005). We have described a method for mucus measurements on intestinal tissue mounted in horizontal Ussing-type chambers, a method useful for analyzing the effects of various drugs and buffer compositions as the mucosal and serosal side of the tissue can be separately exposed (Gustafsson et al., 2012b). Here we show that in CF ileum, the new generation ENaC inhibitors Compound A and AZD5634 detached CF mucus to the same extent as the two NHE inhibitors, DMA and AZ1607. In contrast, the prototypical ENaC inhibitor amiloride had no effect on mucus attachment or surface pH in the ileum at a concentration ten-fold higher than the one causing full ENaC inhibition (Åstrand et al., 2015). Furthermore, the ENaC inhibitors amiloride, Parion and SPX-101 did not increase mucus bundle transport in CF piglet tracheas. The mucus detaching effect of NHE inhibitors and ENaC inhibitors was prevented by apical preincubation with the general anion exchange inhibitor DIDS. Please note that the demonstrated effect of DIDS cannot be via CFTR inhibition, as the experiments were performed in CFTR null animals. Likewise, removal of bicarbonate from the serosal buffer resulted in attached mucus. Together with the fact that the ileum does not express functional ENaC, this is a strong indication that these drugs detach mucus via a mechanism distinct from ENaC inhibition.

We have previously demonstrated that mucus expansion is required for mucus detachment (Gustafsson et al., 2012a; Schütte et al., 2014). The dense packing of mucus in goblet cell granules is achieved by low pH and Ca^{2+} bound to the high affinity binding site in the MUC2 N-terminus (Ambort et al., 2012). Mucus secretion must be accompanied by bicarbonate secretion via CFTR for sufficient mucus expansion, giving the enzyme meprin β access to cleave MUC2 and detach the mucus. Bicarbonate and pH are major regulators of mucus properties, which is evident in CF, where CFTR-function is decreased and the bicarbonate concentration is too low for expansion and detachment of mucus, leading to mucus accumulation. The major ileal NHE, NHE3 (SLC9A3) is an exchanger importing sodium and secreting protons (Tse et al., 1993). Intestinal pH is regulated by NHE3 and inhibition of the exchanger leads to increased luminal bicarbonate concentration and pH (Singh et al., 2013; Tse et al., 1993) via SLC26A3 and A9 activity (Singh et al., 2013). Here we show that NHE3 inhibition by AZ1607 increased the pH in the ileum. Therefore, the pH increase caused by Compound A may also be due to NHE3 inhibition. Based on our own experiments we propose a similar mechanism in the airways. Inhibition of proton secretion via NHE will reduce proton concentration and unmask apical bicarbonate secretion via as yet unidentified bicarbonate transport, potentially sodium/bicarbonate antiporters of the SLC26A family, as has been demonstrated in the intestine. We build this hypothesis on the results that 1) the general anion inhibitor DIDS reversed the effect of NHE inhibitors in the ileum and airways from CFTR null animals and 2) omitting bicarbonate from the basolateral buffer reversed the effect of NHE3 inhibitors in the ileum. Thus, NHE inhibitors increase bicarbonate secretion via existing bicarbonate transporters.

Since the new generation ENaC inhibitors were developed to affect airway pathophysiology, we wanted to compare the effects in the CF ileum to CF airway mucus bundle transport. The piglet model was recently used to show that airways are cleared by mucus bundles (Ermund et al., 2017a) consisting of thousands of linear MUC5B molecules secreted from submucosal glands (Trillo-Muyo et al., 2018). We have observed that the mucus bundles

were immobile in newborn CF piglet airways, demonstrating that CF airway disease is present from birth (Ermund et al., 2018). Our results indicated that ENaC inhibition played a small role for mucus detachment in the airways because amiloride, Parion and SPX-101 were devoid of effect, even though they work via different mechanisms to inhibit ENaC, whereas Compound A and AZD5634 increased CF mucus bundle velocity. In accordance with the hypothesis, Compound A and AZD5634 also caused an increase in surface pH in CF trachea, indicating decreased hydrogen secretion. ENaC inhibition leads to increased liquid secretion and we have shown previously that liquid secretion or increased liquid transport does not necessarily lead to increased mucus bundle transport (Ermund et al., 2018). Instead, an increasing body of evidence points to the importance of bicarbonate via CFTR for formation of normal, non-attached, easily movable mucus (Ermund et al., 2018; Gustafsson et al., 2012a). We have also demonstrated that the concentration of sodium chloride needed to detach CF mucus is at least 300 mM (Ermund et al., 2015b) and we question whether that concentration can be attained by inhibiting ENaC *in vivo*.

Lung function and susceptibility to *Pseudomonas aeruginosa* infection are governed by disease modifier genes in addition to CFTR mutation. Genome-wide association analysis of CF gene modifiers link the sodium/proton exchanger NHE3 (SLC9A3) to meconium ileus (Sun et al., 2012) and lung disease severity (Corvol et al., 2015; Guillot et al., 2014) but how NHE3 modifies CF disease on a mechanistic level is not understood. Based on our quantification of mRNA levels in WT and CF piglet lungs, NHE1 was the isoform with the highest expression. Amiloride at 100 μM inhibits NHE1 (Hirsh et al., 2008), but did not detach CF mucus in the ileum, indicating that inhibition of NHE1 does not cause mucus detachment or alternatively that apical amiloride does not reach NHE1 expressed on the basolateral side. In contrast, amiloride at 100 μM was demonstrated not to inhibit NHE3 (Hirsh et al., 2008), consistent with our results. We found that NHE7 was expressed in piglet lung, and published single cell mRNA sequencing results indicate that NHE7 is enriched in ionocytes, specialized cells enriched in CFTR in both human and mouse airways (Montoro et al., 2018; Plasschaert et al., 2018).

In CF ileum, all drugs tested except amiloride detached the mucus with similar efficacy, whereas Compound A and AZD5634 increased airway mucus bundle transport. The expression of NHE isoforms differs between different organs as NHE3 is abundant in the ileum and NHE6, 7 and 8 were expressed in the lung. Thus, it is reasonable that the demonstrated organ differences in compound sensitivity reflects NHE isoform selectivity of the different compounds. Species differences are also a possible explanation as the intestine was studied in mice and airways in piglets.

The apparent isoform selectivity is also verified by the ability to increase surface pH. Compound A increased luminal pH in both WT and CF ileum as efficiently as the NHE3 inhibitor AZ1607. In contrast, Parion had no effect on surface pH, likely reflecting selectivity toward ENaC compared to the NHE isoforms expressed in ileum and airways. Compound A increased surface pH in WT and CF ileum as well as CF airways, detached mucus in the ileum and increased mucus bundle transport in the airways. AZD5634 had no effect on luminal pH in the ileum but increased surface pH in both WT and CF piglet airway. This observation suggests airway over ileum selectivity for AZD5634, but does not

explain the fact that mucus was detached in the ileum despite lack of pH effects for both Parion and AZD5634. There are further exceptions as amiloride increased airway surface pH but had no effect on mucus bundle transport. Further studies are necessary to fully explore the link between NHE inhibition, luminal pH and mucus detachment. Furthermore, the pH measurements performed here in explants may not reflect *in vivo* values. Because the airways are not covered by a buffering layer such as the mucus layer in the intestine, discrepancies such as some compounds displaying effect on mucus attachment without pH effect, may be explained by methodological difficulties. However, the fact that only two of four new generation ENaC inhibitors increased airway mucus bundle velocity suggests an additional target that should be explored to improve the effect of potential drugs for treatment of CF lung disease.

In conclusion, these observations indicate that inhibition of NHE is required if potential therapies are to detach CF airway mucus, and weak NHE inhibition may explain the previous lack of clinical efficacy by ENaC inhibitors. Further experiments are required to establish what NHE isoforms are expressed in human airways and the most beneficial isoform to inhibit to improve mucus transport and prevent mucus accumulation in CF.

Supplementary Material

Refer to Web version on PubMed Central for supplementary material.

Acknowledgments

Funding

This work was supported by the European Research Council ERC (694181), the Swedish Research Council (2017-00958), The Swedish Cancer Foundation, The Knut and Alice Wallenberg Foundation (2017.0028), IngaBritt and Arne Lundberg Foundation, Sahlgrenska University Hospital (ALF), Wilhelm and Martina Lundgren's Foundation, National Institute of Allergy and Infectious Diseases (U01AI095473, the content is solely the responsibility of the authors and does not necessarily represent the official views of the NIH), The Swedish Foundation for Strategic Research, Erica Lederhausen's Foundation, The Swedish Heart and Lung Foundation (20160241, 20190311), the Swedish Cystic Fibrosis Foundation, Magnus Bergvall´s Foundation, Lederhausen's Center for CF Research at the University of Gothenburg and the Cystic Fibrosis Foundation (CFFT, Hansson14X0; TARRAN17G0).

References

Ambort D, Johansson MEV, Gustafsson JK, Nilsson HE, Ermund A, Johansson BR, Koeck PJB, Hebert H, Hansson GC, 2012. Calcium and pH-dependent packing and release of the gel-forming MUC2 mucin. Proc Natl Acad Sci USA109, 5645–5650. [PubMed: 22451922]

Colombo C, Ellemunter H, Houwen R, Munck A, Taylor C, Wilschanski M, 2011. Guidelines for the diagnosis and management of distal intestinal obstruction syndrome in cystic fibrosis patients. J Cyst Fibros10, S24–S28. [PubMed: 21658638]

Corvol H, Blackman SM, Boëlle P-Y, Gallins PJ, Pace RG, Stonebraker JR, Accurso FJ, Clement A, Collaco JM, Dang H, Dang AT, Franca A, Gong J, Guillot L, Keenan K, Li W, Lin F, Patrone MV, Raraigh KS, Sun L, Zhou Y-H, O'Neal WK, Sontag MK, Levy H, Durie PR, Rommens JM, Drumm ML, Wright FA, Strug LJ, Cutting GR, Knowles MR, 2015. Genome-wide association meta-analysis identifies five modifier loci of lung disease severity in cystic fibrosis. Nature Commun6, 8382. [PubMed: 26417704]

Ermund A, Meiss LN, Dolan B, Bähr A, Klymiuk N, Hansson GC, 2018. The mucin bundles responsible for airway cleaning are retained in cystic fibrosis and by cholinergic stimulation. Eur. Respir. J. 52, pii: 1800457.

Ermund A, Meiss LN, Gustafsson JK, Hansson GC, 2015a. Hyper-osmolarity and calcium chelation: Effects on cystic fibrosis mucus. Eur. J. Pharmacol. 764, 109–117. [PubMed: 26134505]

Ermund A, Meiss LN, Rodriguez-Pineiro AM, Bähr A, Nilsson HE, Trillo-Muyo S, Ridley C, Thornton DJ, Wine JJ, Hebert H, Klymiuk N, Hansson GC, 2017a. The normal trachea is cleaned by MUC5B mucin bundles from the submucosal glands coated with the MUC5AC mucin. Biochem. Biophys. Res. Commun. 492, 331–337. [PubMed: 28859985]

Ermund A, Meiss LN, Scholte BJ, Hansson GC, 2015b. Hypertonic saline releases the attached small intestinal cystic fibrosis mucus. Clin. Exp. Pharmacol. Physiol. 42, 69–75. [PubMed: 25311799]

Ermund A, Recktenwald CV, Skjåk-Bræk G, Meiss LN, Onsøyen E, Rye PD, Dessen A, Myrset AH, Hansson GC, 2017b. OligoG CF-5/20 normalizes cystic fibrosis mucus by chelating calcium. Clin. Exp. Pharmacol. Physiol. 44, 639–647. [PubMed: 28261854]

Ermund A, Schütte A, Johansson MEV, Gustafsson JK, Hansson GC, 2013. The gastrointestinal mucus layers have different properties depending on location within the tract – 1. Studies of mucus in mouse stomach, small intestine, Peyeŕs patches and colon. Am J Physiol Gastrointest Liver Physiol305, G341–347. [PubMed: 23832518]

Fukushima K, Sato S, Naito H, Funayama Y, Haneda S, Shibata C, Sasaki I, 2005. comparative study of epithelial gene expression in the small intestine among total proctocolectomized, dietary sodium-depleted, and aldosterone-infused rats. J. Gastrointest. Surg. 9, 236–244. [PubMed: 15694820]

Furukawa O, Bi LC, Guth PH, Engel E, Hirokawa M, Kaunitz JD, 2004. NHE3 inhibition activates duodenal bicarbonate secretion in the rat. Am J Physiol Gastrointest Liver Physiol286, G102–G109. [PubMed: 12881227]

Guillot L, Beucher J, Tabary O, Le Rouzic P, Clement A, Corvol H, 2014. Lung disease modifier genes in cystic fibrosis. Int. J. Biochem. Cell Biol. 52, 83–93. [PubMed: 24569122]

Gustafsson JK, Ermund A, Ambort D, Johansson MEV, Nilsson HE, Thorell K, Hebert H, Sjövall H, Hansson GC, 2012a. Bicarbonate and functional CFTR channel are required for proper mucin secretion and link cystic fibrosis with its mucus phenotype. J. Exp. Med. 209, 1263–1272. [PubMed: 22711878]

Gustafsson JK, Ermund A, Johansson MEV, Schütte A, Hansson GC, Sjövall H, 2012b. An ex vivo method for studying mucus formation, properties, and thickness in human colonic biopsies and mouse small and large intestinal explants. Am J Physiol Gastrointest Liver Physiol302, G430–G438. [PubMed: 22159279]

Hasselblatt P, Warth R, Schulz-Baldes A, Greger R, Bleich M, 2000. pH regulation in isolated in vitro perfused rat colonic crypts. Pflugers Arch. 441, 118–124. [PubMed: 11205049]

Hirsh AJ, Zhang J, Zamurs A, Fleegle J, Thelin WR, Caldwell RA, Sabater JR, Abraham WM, Donowitz M, Cha B, Johnson KB, St. George JA, Johnson MR, Boucher RC, 2008. Pharmacological Properties of N-(3,5-Diamino-6-chloropyrazine-2-carbonyl)-N′−4-[4-(2,3-dihydroxypropoxy)phenyl]butyl-guanidine Methanesulfonate (552–02), a Novel Epithelial Sodium Channel Blocker with Potential Clinical Efficacy for Cystic Fibrosis Lung Disease. J. Pharmacol. Exp. Ther. 325, 77–88. [PubMed: 18218832]

Klymiuk N, Mundhenk L, Kraehe K, Wuensch A, Plog S, Emrich D, Langenmayer MC, Stehr M, Holzinger A, Kröner C, Richter A, Kessler B, Kurome M, Eddicks M, Nagashima H, Heinritzi K, Gruber AD, Wolf E, 2012. Sequential targeting of CFTR by BAC vectors generates a novel pig model of cystic fibrosis. J. Mol. Med. 90, 597–608. [PubMed: 22170306]

Koyama K, Sasaki I, Naito H, Funayama Y, Fukushima K, Unno M, Matsuno S, Hayashi H, Suzuki Y, 1999. Induction of epithelial Na+channel in rat ileum after proctocolectomy. Am J Physiol Gastrointest Liver Physiol276, G975–G984.

Masereel B, Pochet L, Laeckmann D, 2003. An overview of inhibitors of Na+/H+ exchanger. Eur J Med Chem38, 547–554. [PubMed: 12832126]

Montoro DT, Haber AL, Biton M, Vinarsky V, Lin B, Birket SE, Yuan F, Chen S, Leung HM, Villoria J, Rogel N, Burgin G, Tsankov AM, Waghray A, Slyper M, Waldman J, Nguyen L, Dionne D, Rozenblatt-Rosen O, Tata PR, Mou H, Shivaraju M, Bihler H, Mense M, Tearney GJ, Rowe SM, Engelhardt JF, Regev A, Rajagopal J, 2018. A revised airway epithelial hierarchy includes CFTR-expressing ionocytes. Nature560, 319–324. [PubMed: 30069044]

Moore PJ, Tarran R, 2018. The epithelial sodium channel (ENaC) as a therapeutic target for cystic fibrosis lung disease. Expert Opin Ther Targets22, 687–701. [PubMed: 30028216]

Plasschaert LW, Žilionis R, Choo-Wing R, Savova V, Knehr J, Roma G, Klein AM, Jaffe AB, 2018. A single-cell atlas of the airway epithelium reveals the CFTR-rich pulmonary ionocyte. Nature560, 377–381. [PubMed: 30069046]

Repishti M, Hogan DL, Pratha V, Davydova L, Donowitz M, Tse CM, Isenberg JI, 2001. Human duodenal mucosal brush border Na+/H+ exchangers NHE2 and NHE3 alter net bicarbonate movement. Am J Physiol Gastrointest Liver Physiol281, G159–G163. [PubMed: 11408268]

Rowe SM, Clancy JP, Wilschanski M, 2011. Nasal Potential Difference Measurements to Assess CFTR Ion Channel Activity, in: Amaral MD, Kunzelmann K. (Eds.), Cystic Fibrosis: Diagnosis and Protocols, Volume I: Approaches to Study and Correct CFTR Defects. Humana Press, Totowa, NJ, pp. 69–86.

Sathe M, Houwen R, 2017. Meconium ileus in Cystic Fibrosis. J Cyst Fibros16, S32–S39. [PubMed: 28986020]

Schütte A, Ermund A, Becker-Pauly C, Johansson MEV, Rodriguez-Pineiro AM, Bäckhed F, Müller S, Lottaz D, Bond JS, Hansson GC, 2014. Microbial-induced meprin β cleavage in MUC2 mucin and a functional CFTR channel are required to release anchored small intestinal mucus. Proc Natl Acad Sci USA111, 12396–12401. [PubMed: 25114233]

Scott DW, Walker MP, Sesma J, Wu B, Stuhlmiller TJ, Sabater JR, Abraham WM, Crowder TM, Christensen DJ, Tarran R, 2017. SPX-101 Is a Novel Epithelial Sodium Channel–targeted Therapeutic for Cystic Fibrosis That Restores Mucus Transport. Am. J. Respir. Crit. Care Med. 196, 734–744. [PubMed: 28481660]

Simonin J, Bille E, Crambert G, Noel S, Dreano E, Edwards A, Hatton A, Pranke I, Villeret B, Cottart C-H, Vrel J-P, Urbach V, Baatallah N, Hinzpeter A, Golec A, Touqui L, Nassif X, Galietta LJV, Planelles G, Sallenave J-M, Edelman A, Sermet-Gaudelus I, 2019. Airway surface liquid acidification initiates host defense abnormalities in Cystic Fibrosis. Sci Rep9, 6516. [PubMed: 31019198]

Singh AK, Liu Y, Riederer B, Engelhardt R, Thakur BK, Soleimani M, Seidler U, 2013. Molecular transport machinery involved in orchestrating luminal acid-induced duodenal bicarbonate secretion in vivo. J Physiol591, 5377–5391. [PubMed: 24018950]

Sun L, Rommens JM, Corvol H, Li W, Li X, Chiang TA, Lin F, Dorfman R, Busson P-F, Parekh RV, Zelenika D, Blackman SM, Corey M, Doshi VK, Henderson L, Naughton KM, O'Neal WK, Pace RG, Stonebraker JR, Wood SD, Wright FA, Zielenski J, Clement A, Drumm ML, Boëlle P-Y, Cutting GR, Knowles MR, Durie PR, Strug LJ, 2012. Multiple apical plasma membrane constituents are associated with susceptibility to meconium ileus in individuals with cystic fibrosis. Nat. Genet. 44, 562. [PubMed: 22466613]

Trillo-Muyo S, Nilsson HE, Recktenwald CV, Ermund A, Ridley C, Meiss LN, Bahr A, Klymiuk N, Wine JJ, Koeck PJ, Thornton DJ, Hebert H, Hansson GC, 2018. Granule-stored MUC5B mucins are packed by the non-covalent formation of N-terminal head-to-head tetramers. J. Biol. Chem. 293, 5746–5754. [PubMed: 29440393]

Tse CM, Levine SA, Yun CH, Brant SR, Pouyssegur J, Montrose MH, Donowitz M, 1993. Functional characteristics of a cloned epithelial Na+/H+ exchanger (NHE3): resistance to amiloride and inhibition by protein kinase C. Proc Natl Acad Sci USA90, 9110–9114. [PubMed: 8415663]

Turner JR, Black ED, Ward J, Tse C-M, Uchwat FA, Alli HA, Donowitz M, Madara JL, Angle JM, 2000. Transepithelial resistance can be regulated by the intestinal brush-border Na+/H+ exchanger NHE3. Am J Physiol Cell Physiol279, C1918–C1924. [PubMed: 11078707]

van Doorninck JH, French PJ, Verbeek E, Peters HHPC, Morreau H, Bijman J, Scholte B, 1995. A mouse model for the cystic fibrosis delta F508 mutation. EMBO J. 14, 4403–4411. [PubMed: 7556083]

Åstrand ABM, Hemmerling M, Root J, Wingren C, Pesic J, Johansson E, Garland AL, Ghosh A, Tarran R, 2015. Linking increased airway hydration, ciliary beating, and mucociliary clearance through ENaC inhibition. Am J Physiol Lung Cell Mol Physiol308, L22–L32. [PubMed: 25361567]

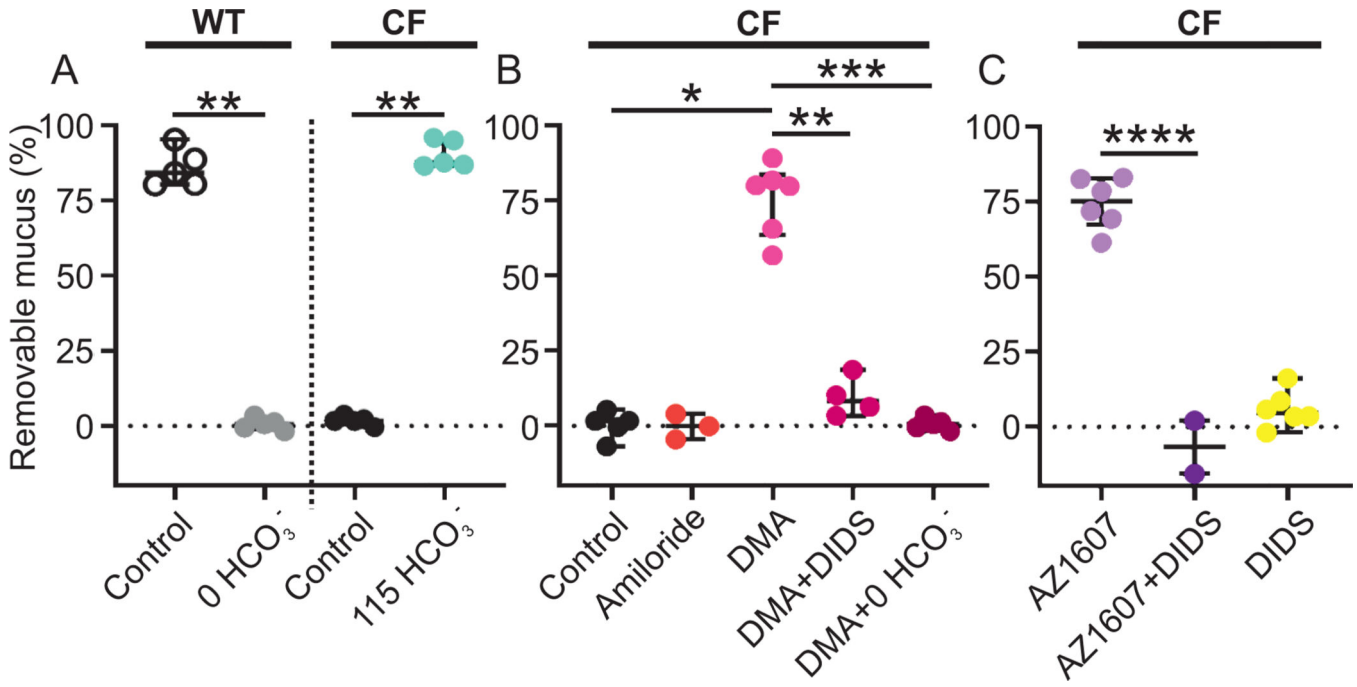

Figure 1. Attached CF mucus is detached by bicarbonate and NHE3 inhibition.

(A) Mucus is easily aspirated in WT mouse ileum (WT control median 84.3%, n = 5) but attached in WT mouse ileum perfused with buffer without bicarbonate (WT 0 HCO_3^- median 0.56%, n = 5), ** P = 0.008, Mann-Whitney U-test. Mucus is also attached in CF mouse ileum (CF control median 1.66%, n = 5) but is detached by 115 mM bicarbonate (CF 115 HCO_3^- median 8.87%, n = 5), ** P = 0.008, Mann-Whitney U-test. The pH of all buffers was 7.4. The buffer with 115 mM bicarbonate had a Cl^- concentration of 9 mM. All other buffers contained 23 mM bicarbonate and 120 mM Cl^-. Data presented as median ± interquartile range.

(B) Apical incubation with 100 μM amiloride in CF ileum (median −0.13%, n = 3) did not detach CF mucus (median 1.61%, n = 5). The sodium/proton exchange (NHE) inhibitor dimethyl-amiloride (DMA) detached CF mucus when incubated at 100 μM apically (median 80.0%, n = 6), * P = 0.01, Kruskal-Wallis and Dunńs multiple comparisons test. The detaching effect of DMA was reversed by apical preincubation for 30 min with the general anion transport inhibitor DIDS at 100 μM (median 81.8%, n = 4), ** P = 0.01, Mann-Whitney U-test and the same effect was achieved by perfusing the explant with bicarbonate free buffer on the serosal side (median 0.56%, n = 5), *** P = 0.0008, Kruskal-Wallis and Dunńs multiple comparisons test. Data presented as median ± interquartile range.

(C) A more potent NHE3 inhibitor, AZ1607 at 300 nM, had the same detaching effect as DMA (median 75.2%, n = 6), ** P = 0.004, Mann-Whitney U-test and was also reversed by apical preincubation with DIDS (median −6.81%, n = 2) ****P < 0.0001, t-test. Mucus attachment was not affected by DIDS alone (median 4.63%, n = 6). Data presented as median ± interquartile range. For compound molecular structures, see Figure S1.

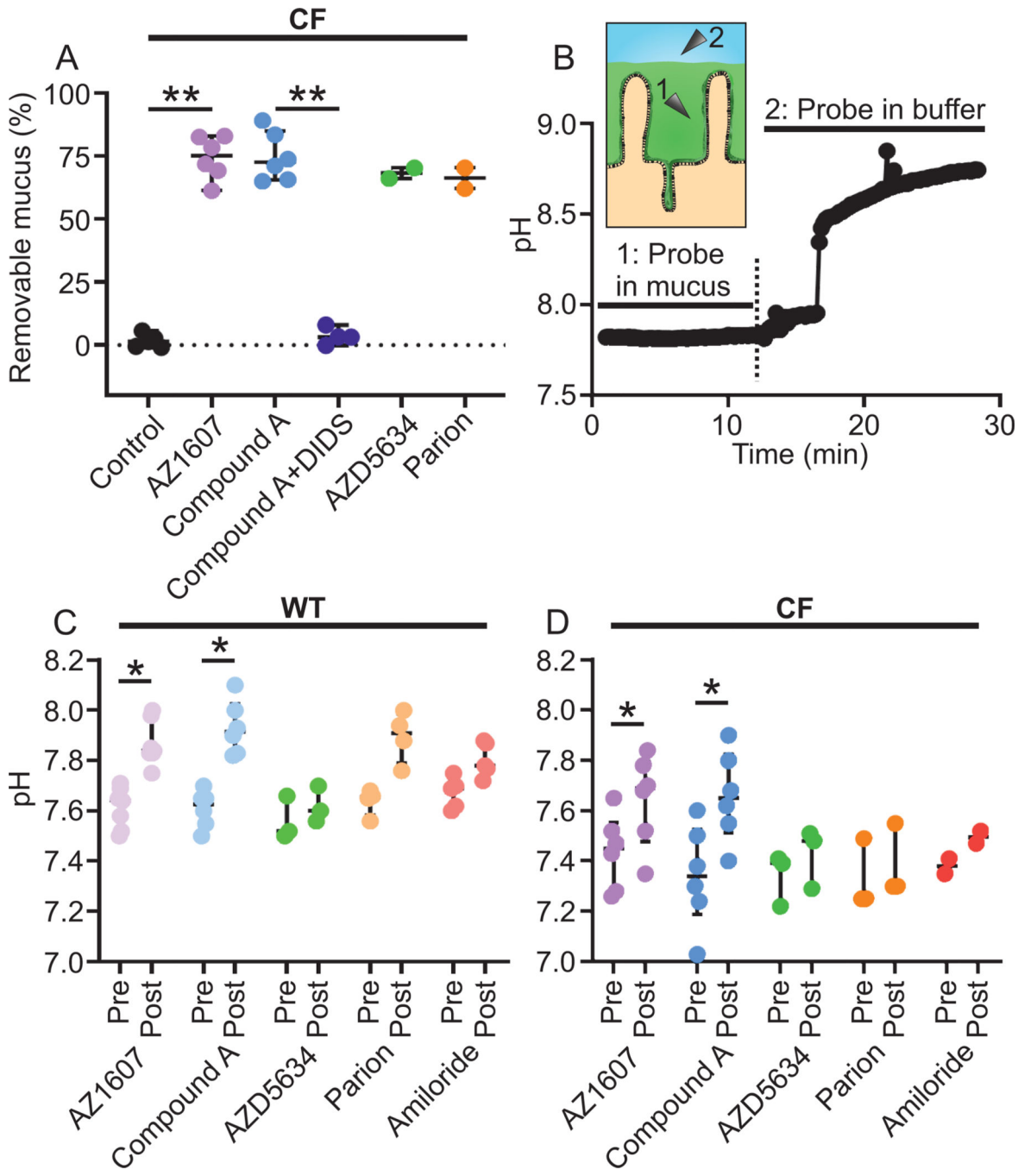

Figure 2. New generation ENaC inhibitors detach CF mucus in the mouse ileum.

(A) The NHE3 inhibitor AZ1607 (300 nM) detached CF mucus (median 75.2%, n = 6), ** P = 0.004, Mann-Whitney U-test. The ENaC inhibitor Compound A at 1 μM detached mucus in CF ileum (median 72.5%, n = 6), ** P = 0.003, Kruskal-Wallis and Dunńs multiple comparisons test and again the effect was reversed by apical preincubation with DIDS at 100 μM (median 3.19%, n = 4), ** P = 0.01, Mann-Whitney U-test. The detaching effect was present with two other ENaC inhibitors, AZD5634, median 68.3% and Parion, median 66.3%, both at 1 μM (n = 2 in each group). Data presented as median ± interquartile range.

(B) Principle for mucosal pH measurements in the mouse ileum. The mucus layer in the ileum (green, 1) maintains a stable pH at the epithelial surface whereas the pH in the buffer (blue, 2) is less stable and reflects buffer pH.
(C) In WT, both the NHE3 inhibitor AZ1607 (median change 0.26 pH units, n = 7, * P = 0.02) and the ENaC inhibitor Compound A at 1 μM (median change 0.30, n = 6, * P = 0.03) increased surface pH. Parion (n = 4) did not increase the pH, Wilcoxon signed-rank test. Pre and Post denote before and after addition of indicated compound to the apical buffer. The post-measurement was taken when the plateau was reached. Data presented as median ± interquartile range.
(D) In CF, both AZ1607 (median change 0.20 pH units, n = 6, * P = 0.02) and Compound A (median change 0.31, n = 6, * P = 0.03) increase surface pH, Wilcoxon signed-rank test. Pre and Post denote before and after addition of indicated compound to the apical buffer. The post-measurement was taken when the plateau was reached. Data presented as median ± interquartile range.

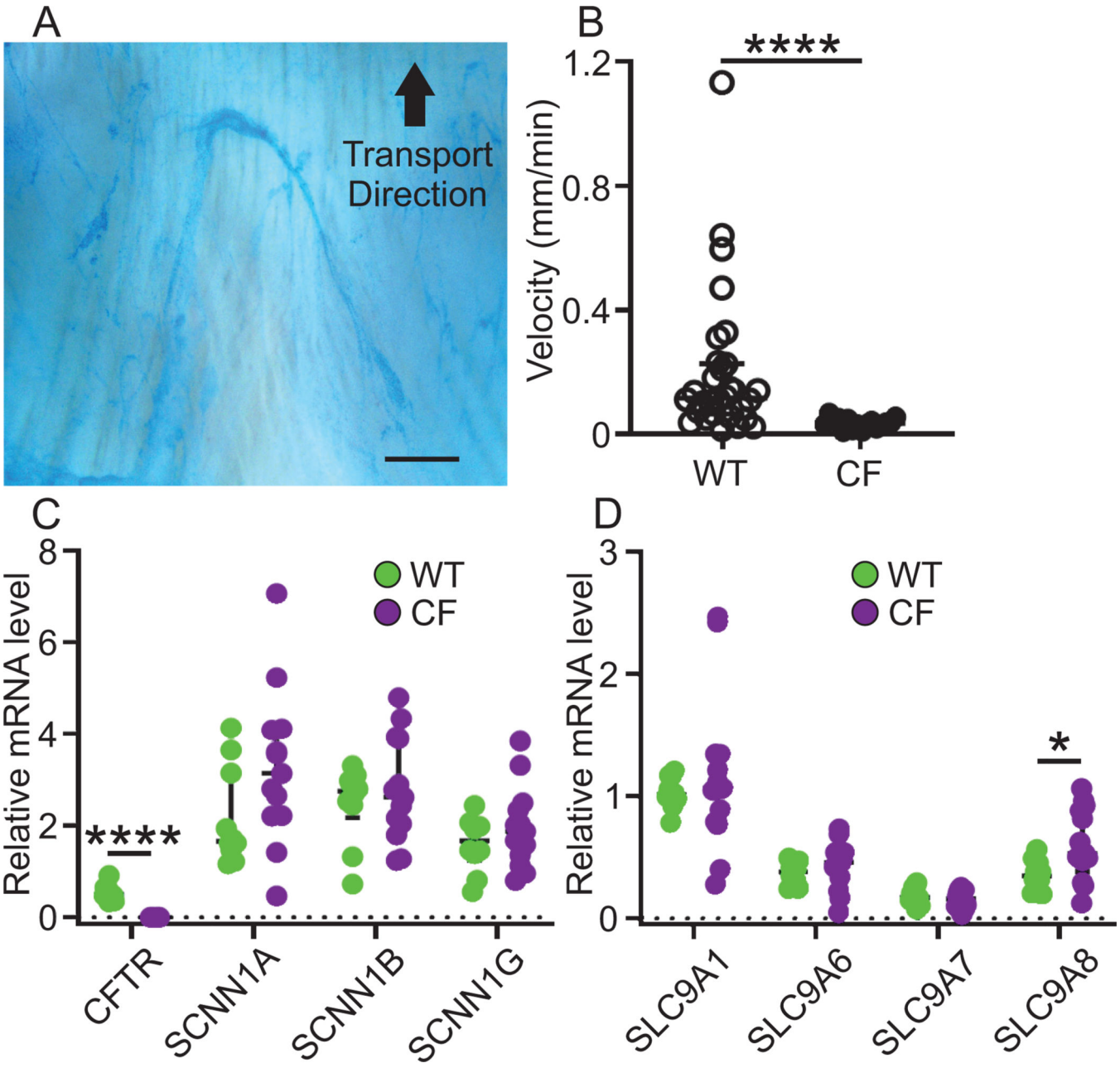

Figure 3. Newborn piglet airways are cleared by mucus bundles and express NHE mRNA.

(A) Transport velocity of mucus bundles consisting of linear MUC5B secreted from submucosal glands was quantified by measuring transport of Alcian blue stained bundles in time lapse recordings. Scale bar: 300 μm.

(B) The bundles clear the airway surface in WT airways (median velocity 0.12 mm/min, n = 30 piglets) but are immobile in CF airways (median velocity 0.034 mm/min, n = 16 piglets), **** $P < 0.0001$, Mann-Whitney U-test. Data presented as median ± interquartile range.

(C) Quantitative PCR of mRNA prepared from piglet lung tissue revealed that the mRNA level for CFTR was significantly higher in WT (n = 10 piglets) compared to CF (n = 13 piglets) lungs **** $P < 0.0001$, Mann-Whitney U-test. The mRNA levels of ENaC subunits

SCNN1A, SCNN1B and SCNN1G were similar in WT and CF piglet lungs, WT (n = 10 piglets) and CF (n = 13 piglets). Data expressed as median ± interquartile range. See also Figure S2.

(D) The mRNA level for SLC9A1 was the highest among the SLC9A family and the second highest levels were detected for SLC9A8. There was no difference in expression between WT (n = 10 piglets) and CF (n = 13 piglets) except for SLC9A8, which was higher in CF, * P = 0.04, Mann-Whitney U-test. Data expressed as median ± interquartile range. See also Figure S2.

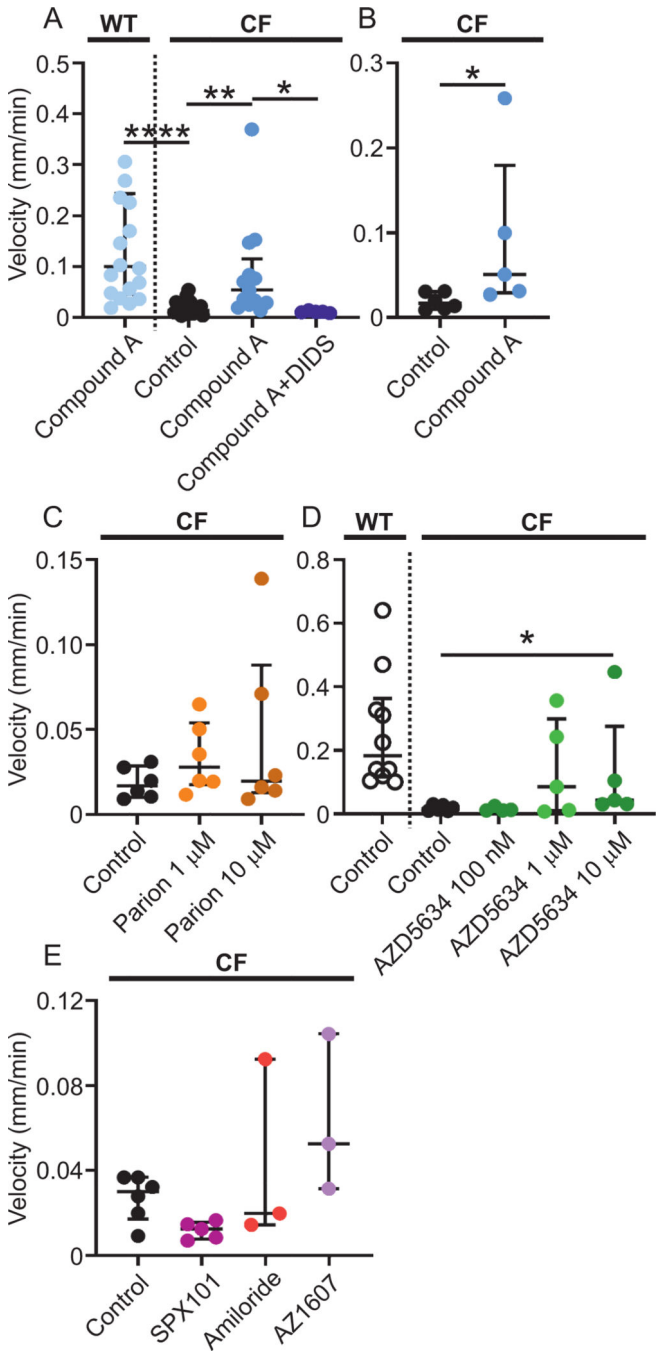

Figure 4. New generation ENaC inhibitors increase mucus bundle transport in CF piglet airways.

(A) Mucus bundle transport in WT piglet airways after preincubation with the ENaC inhibitor Compound A at 1 µM (WT Compound A median velocity 0.10 mm/min, n = 18 time lapses, 9 piglets) was substantially higher than mucus bundle transport in CF piglets (CF control median velocity 0.014 mm/min, n = 20 time lapses, 6 piglets), **** P < 0.0001, Kruskal-Wallis and Dunńs multiple comparisons test. Preincubation with Compound A (median velocity 0.054 mm/min, n = 13 time lapses, 5 piglets) increased the mucus bundle transport in CF piglet airways ** P = 0.002, Kruskal-Wallis and Dunńs multiple

comparisons test. This increase was reversed by 100 μM DIDS (median velocity 0.012 mm/min, n = 5 time lapses, 1 piglet) * P = 0.015, Kruskal-Wallis and Dunńs multiple comparisons test. Data presented as median ± interquartile range.

(B) Mucus bundle transport was lower in CF control (median velocity 0.017 mm/min, n = 6 piglets) compared to transport after preincubation with Compound A in CF piglet airways (median velocity 0.051 mm/min, n = 5 piglets) * P = 0.017, Mann-Whitney U-test also when comparing the means of each pig instead of each time lapse. Data presented as median ± interquartile range.

(C) The ENaC inhibitor Parion had no effect on mucus bundle velocity at 1 μM or at 10 μM (CF control median velocity 0.017 mm/min, n = 6 piglets, Parion 1 μM median velocity 0.028 mm/min, n = 6 piglets, Parion 10 μM median velocity 0.020 mm/min, n = 6 piglets), Kruskal-Wallis and Dunńs multiple comparisons test. Data presented as median ± interquartile range.

(D) Mucus transport was faster in WT than CF without treatment (WT Control median velocity 0.18 mm/min, n = 10 piglets, CF Control median velocity 0.017 mm/min, n = 6 piglets). The ENaC inhibitor AZD5634 had no effect at 100 nM (median velocity 0.012 mm/min, n = 4 piglets) or at 1 μM (median velocity 0.086 mm/min, n = 5 piglets) but increased mucus bundle velocity at 10 μM (median velocity 0.044 mm/min, n = 5 piglets), * P = 0.04, Kruskal-Wallis and Dunńs multiple comparisons test. Data presented as median ± interquartile range.

(E) The ENaC inhibitors SPX101 (10 μM) and amiloride (100 μM) as well as the NHE3 inhibitor AZ1607 (300 nM) had no effect on mucus bundle velocity (CF Control median velocity 0.03 mm/min, n = 6 piglets, CF SPX101 median velocity 0.013 mm/min, n = 5 piglets, CF amiloride median velocity 0.02 mm/min, n = 3 piglets, CF AZ1607 median velocity 0.05 mm/min, n = 3 piglets), Kruskal-Wallis and Dunńs multiple comparisons test. Data presented as median ± interquartile range.

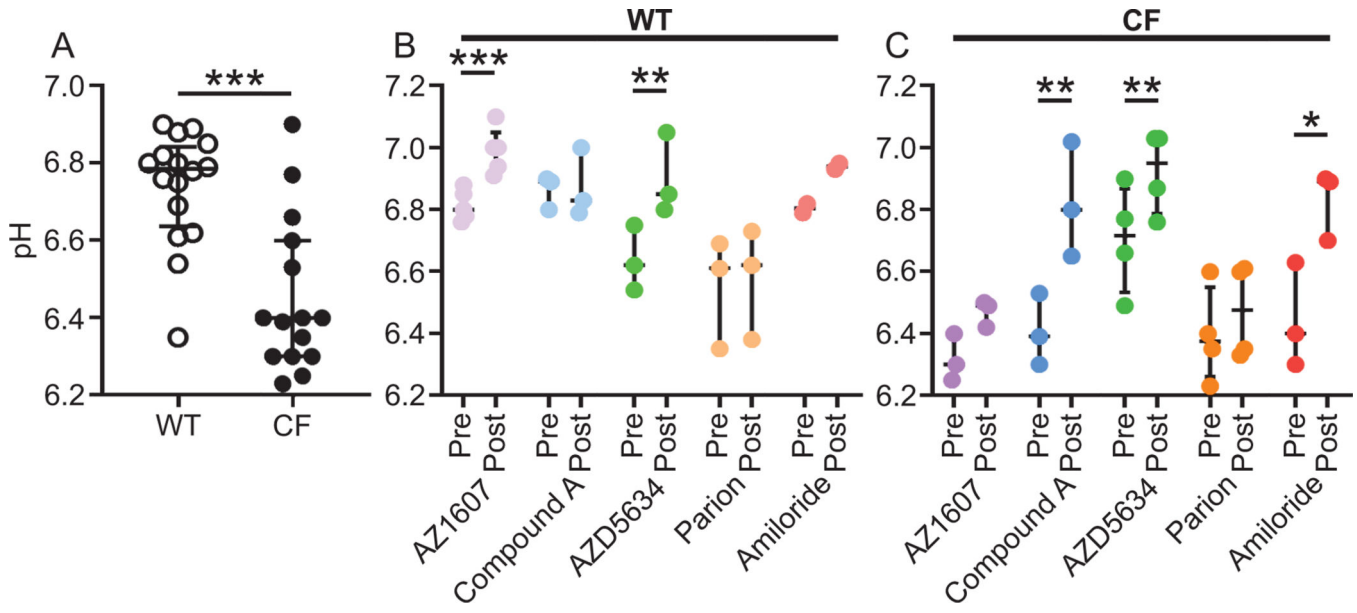

Figure 5. New generation ENaC inhibitors increase surface pH in piglet trachea.

(A) The airway surface pH was measured with microelectrodes in WT (median 6.79 pH units, n = 16 piglets) and CF (median 6.40 pH units, n = 15 piglets). The pH was higher in WT than CF piglet airways, *** P = 0.0003, Mann-Whitney U-test. Data presented as median ± interquartile range.

(B). In WT piglet trachea, the NHE3 inhibitor AZ1607 (median change 0.18 pH units, 300 nM, n = 5 piglets) increased the pH *** P = 0.0004. The ENaC inhibitors Compound A (1 μM, n = 3 pigs), Parion (1 μM, n = 3 piglets) and amiloride (100 μM, n = 2 piglets) were without effect on surface pH. In contrast, the ENaC inhibitor AZD5634 (median change 0.26 pH units, 1 μM, n = 3 piglets) increased surface pH, ** P = 0.006, paired t-test. Data presented as median ± interquartile range.

(C) In CF piglet trachea, the NHE3 inhibitor AZ1607 (n = 3 piglets) had no effect on surface pH. In contrast, the ENaC inhibitors Compound A (median change 0.41 pH units, n = 3 piglets, ** P = 0.01), AZD5634 (median change 0.24 pH units, n = 4 piglets, ** P = 0.006) and amiloride (n = 3 piglets, * P = 0.03) increased surface pH. The ENaC inhibitor Parion (median change 0.40 pH units, n = 4 piglets) was without effect, paired t-test. Data presented as median ± interquartile range.

Table 1.

Primer sequences for quantification of mRNA levels.

Gene name	Forward primer (5´ – 3´)	Reverse primer (5´ – 3´)
TBP	GATGGACGTTCGGTTTAGG	AGCAGCACAGTACGAGCAA
GAPDH	CAGAACATCATCCCTGCTTC	GCTTCACCACCTTCTTGATG
YWHAZ	GCATTATTAGCGTGCTGTCTT	ATGCAACCAACACATCCTATC
CFTR	AACCTGAACAAGTTTGATGAAG	AAGGCAAGTCCACAGAAGGC
SCNN1A	GCTTCCAACTGTGCAACCAG	GAGACCTGGTTGAAGCGACA
SCNN1B	CTCCTGCTTCCAAGAGCACA	GGACTCCTTGCAGACGTCAA
SCNN1G	TGGTTGCTGTCTGTTCTCAC	GGATCTCTGGTTCAGGTCTTTG
SLC9A1	CACTGGAAGGACAAGCTCAA	GCCTGCTTCATCTCCATCTT
SLC9A2	GGCAGAGACTGGGATGATAAG	TCGCTGACGGATTTGATAGAG
SLC9A3	CTCAGTGCTCATCCTGCACA	CCAGTGCCACTTCTACCCAG
SLC9A4	CGCTGCTGCATTCTTAGCTG	ATTTCCAAAGCCCCTCCTGG
SLC9A6	TCTTTTGCAATGGGTGCTGC	CAAGAGGAAGGTGCTCCAGG
SLC9A7	TCGCGACCTGAAAACATCCA	CCTGTTGTGGTCACGCAAAG
SLC9A8	CCATCGTCCTGACCAACACA	TTAAGCCAGTGAGAGTGCCG